Connecting communities. Creating resilience.

Physical modelling for mapping firebrand and heat flux on structures in the wildland-urban interface (WUI)

Mr Amila Wickramasinghe

Victoria University

Mapping Firebrand and Heat Flux on Structures in the Forest Dominant Wildland Urban Interface Using Physics-based Modelling

Amila Wickramasinghe[1]; Nazmul Khan[1]; Alexander Filkov[2], Khalid Moinuddin[1]

[1]*Institute for Sustainable Industries and Livable Cities, Victoria University, Melbourne, VIC 3030, Australia {p.wickramasinghe@live.vu.edu.au; Nazmul.khan@vu.edu.au; Khalid.Moinuddin@vu.edu.au}*

[2] *School of Ecosystem and Forest Sciences, Faculty of Science, University of Melbourne, VIC 3363, Australia, {alexander.filkov@unimelb.edu.au}*

Abstract

Firebrands may cause huge destruction to the properties at the wildland-urban interface (WUI) during wildfires. However, Australian Building Standard AS3959 is developed based on radiation heat flux and it does not quantify the effects of firebrand landing flux on structures. To improve the assessment of the Bushfire Attack Level (BAL), there is a need for such quantification. In this study, we aim to quantify the firebrand flux through physical modelling so that the effects of fires, weather conditions, vegetation types and wind speeds are considered simultaneously. A Eucalyptus Forest is modelled as the vegetation species with given understory and canopy fuel loads. Fire Danger Indices (FFDI) of 100, 80, and 50 are used to apply different fire severities. The wind speed is adjusted while keeping the temperature, relative humidity, and drought factor as constants to obtain the focused FFDIs. The surface fires are prescribed and the firebrand size, shape, and quantity are taken from our previous firebrand generation study (Wickramasinghe et al. 2022). The distances between the structure and the vegetation are maintained as per the BAL of AS3959. The radiative heat fluxes correlated to the BALs are obtained with the algorithm provided in AS3959. The findings reveal a logarithmic relationship exists between firebrand flux and radiative heat flux in the range of R^2 0.96 to 0.99. Hence, for a certain BAL, the firebrand flux increases with the FFDI similar to radiative heat flux. Results from this study can be used to quantify the firebrand flux on houses from forest fires, which may improve the design standards and construction requirements to mitigate the vulnerability of structures at WUI.

Keywords**:** physics-based modelling; wildland fire; firebrands; FDS; wildland-urban interface

Introduction

The firebrands generated from burning vegetation are capable of carrying adequate heat to a distance and initiating spot fires (secondary ignitions) after landing on a fuel bed or a structure. Depending on the firebrand material, size, the number of firebrands accumulation, state of firebrand at impact (glowing or flaming), the nature of the spotting surface etc. [1], the ignition potential is varied. Post-fire investigations [2] and some studies [3] claim that firebrands are the main cause of structure ignition in the Wildland Urban Interface. A few fire and building standards specified for different jurisdictions propose precautions to mitigate the vulnerability of structures due to firebrand attacks. The FireSmart Guidebook [4,5] suggests a buffer zone to maintain the degree of vegetation around Canadian buildings to reduce the spotting of sparking and burning firebrands on roofs. The construction material selection for exterior siding, vents, and other openings of the buildings is also included in this standard. The US National Fire Protection Association standards (NFPA) present provisions for firebrand hazard definition by setting up house ignition zones as Immediate zone (0-5 ft from the house), Intermediate zone (5 to 30 ft), and Extended zone (30 to 100 ft) and landscape and vegetation management to reduce firebrand ignition following Cohen et al. [6] structure ignition experiments. Although the fire code of New Zealand [7], Italy [8], and code

Forestier [9] of France set up plans to reduce wildfire risk, do not specify steps to quantify the firebrand attack on structures. The Australian building standard AS3959 [10] qualitatively presents the firebrand attack on houses in the WUI as increased with the Bushfire Attack Level (BAL). BAL is the scale of wildfire risk on houses which is expressed in terms of the radiative heat flux as decreased with increasing the distance between the vegetation edge and the site. In the present study, we mainly quantify the firebrand flux (the number of particles/pieces [pcs] that land on a unit area per unit time [pcs m^{-2} s^{-1}]) at a forest dominant WUI using physics-based modelling.

Methodology

We use the CFD-based Fire Dynamics Simulator [11] which is a product of National Standards Technology, the USA as the modelling tool. FDS numerically solves the governing equations of fire-driven fluid flows and the gas phase is simulated by Large Eddy Simulations (LES). The firebrands are introduced in the domain by Lagrangian particle-based transport scheme.

The length, width and height of the domain are taken as 336 m, 102 m, and 90 m respectively to include an open land for wind flow development, a region to replicate a 40 m tall forest with 25 t ha^{-1} understorey and 10 t ha^{-1} canopy fuel loads as per AS3959 [10], and an area to position a modelled house according to BAL as illustrated in Fig. 1. The eddies of the wind field are added according to Jarrin et al. [12] and the area where wind development happens maintained a 1.5 m grid resolution. The region of fireline, firebrand generation, firebrand transport and spotting is maintained at a 0.75 m grid size as per the grid sensitivity study of Wickramasinghe et al. [13]. The wind velocity at 10 m height U_{10} is varied to obtain Forest Fire Danger Indices (*FFDI*) of 100, 80, and 50 while keeping drought factor (*D*), relative humidity (*Rh*) and ambient temperature (*T*) as constants as per in Eq.1[14]:

$$FFDI = 2.0 \times \exp\left(-0.450 + 0.987 \times \ln(D) - 0.0345 \times Rh + 0.0338 \times T + 0.0234 \times U_{10}\right) \quad \textbf{Eq. 1}$$

The fireline intensities of 54.4, 43.1, and 27 MW m^{-1} to match the FFDIs are calculated accounting for the total fuel load of the forest (35 t ha^{-1}) [10], rate of spread (ROS) of the fire and the heat of combustion (HoC) of the vegetation material. The dominant fuel of the forest vegetation classification is chosen as Eucalyptus [10] according to AS3959. The dimensions and thermophysical properties of fuel particles are taken from the literature [15,16]. The length of the fireline is taken as 100 m [10] and the fireline depth is calculated according to the ROS and the residence time.

The base information of the firebrand generation rate of 4.18 pcs MW^{-1} s^{-1} is taken from Wickramasinghe et al.[13] which was for Pitch Pine vegetation at 31% fuel moisture content (FMC) and 2 m/s average wind velocity at U_{10}. We calibrated the base firebrand generation rate accounting for the effect of wind speeds, FMC, and fuel species with some tree burning experimental studies by Hudson et al.[17] and Bahrani et al. [18]. We formulated these experimental data to find correlations between firebrand generation number and wind, FMC, and fuel species. With the obtained mathematical formulas, the firebrand generation numbers are calculated for known wind speeds (related to FFDI 50, 80, and 100), FMC (3.84%), and Eucalyptus vegetation species as 8.43, 10.68, and 10.68 pcs MW^{-1} s^{-1} to use as firebrand generation source terms of the model. The firebrands are randomly initiated in the tree volume which engulfs by the flame as shown in Fig. 1.

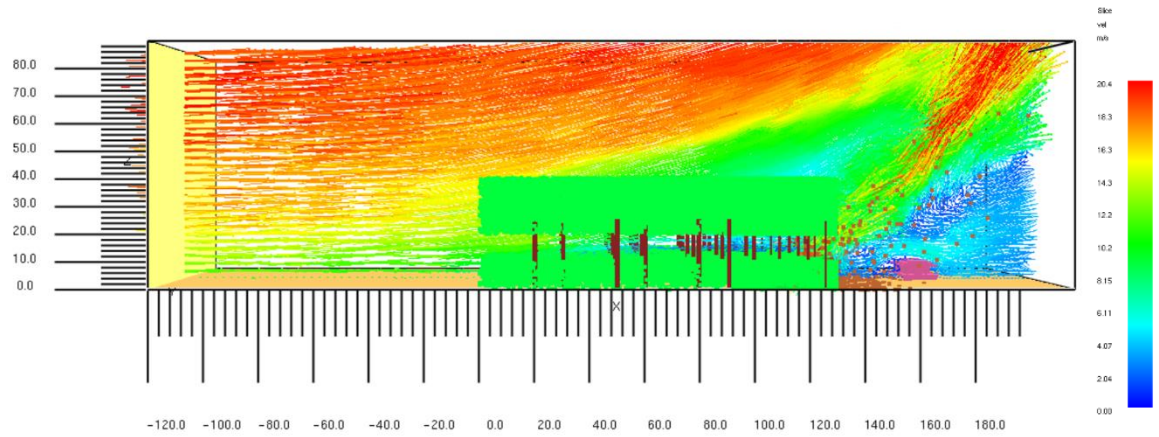

Fig. 1. The simulation domain of Forest fire in FDI 50 and BAL 12.5. The velocity vector slice at Y=0 is presented. The firebrands are initiated at the volume engulfed by the fire and follow the path of fire-induced buoyancy and the wind.

A house is modelled including features such as roof, gutters, deck, sub-floor etc. following a standard house design [19] proposed by the Australian government and positioned according to the BAL. The maximum view factor and corresponding flame angle are calculated according to the performance-based algorithm [10] provided in AS3959 and used to find the emissive power and the theoretical radiative heat flux on the house to compare with the simulations. Devices are set up to capture the firebrand landing number on the total house volume and at the individual strategic locations (roof, gutters, etc.) as time progressed. The firebrand mass distribution is obtained by setting FDS devices in the downwind direction that record mass flux. A total of 15 simulations are conducted by varying the three FFDIs and the five BALs as presented in Table 1[10].

Table 1 The distance from the forest edge to the house for FFDI 100, 80, and 50

FFDI	Bushfire Attack Level (BAL)				
	BAL FZ	**BAL 40**	**BAL 29**	**BAL 19**	**BAL 12.5**
	Distance (m) of the site from the predominant vegetation class				
FFDI 100	<19	19 ≤ 25	25 ≤ 35	31 ≤ 42	48 ≤ 100
FFDI 80	<16	16 ≤ 21	21 ≤ 31	35 ≤ 48	42 ≤ 100
FFDI 50	<12	12 ≤ 16	16 ≤ 23	23 ≤ 32	32 ≤ 100

Results and Discussion

The FDS companion software smokeview shows the originated firebrands lift by the fire-induced buoyancy and transported by the horizontal wind until land on the ground or the modelled house. Depending on the instant resulting force derived from the buoyancy force, drag force and gravitational force, firebrands show different trajectories. Fig. 2 (a) shows the firebrand distribution in the downwind direction for the focused FFDIs. The mass of firebrands landed at a unit time is exponentially decreasing with the distance. The highest firebrand landing occurred for FFDI 100 at the nearest region to the forest edge followed by FDI 80 and 50. This pattern is similar to the number of firebrands generated at the burning vegetation. The amount of firebrands received for FFDI 50 is nearly half of that amount of FFDI 100. According to this, the firebrand attack decreases with the distance and the FFDI.

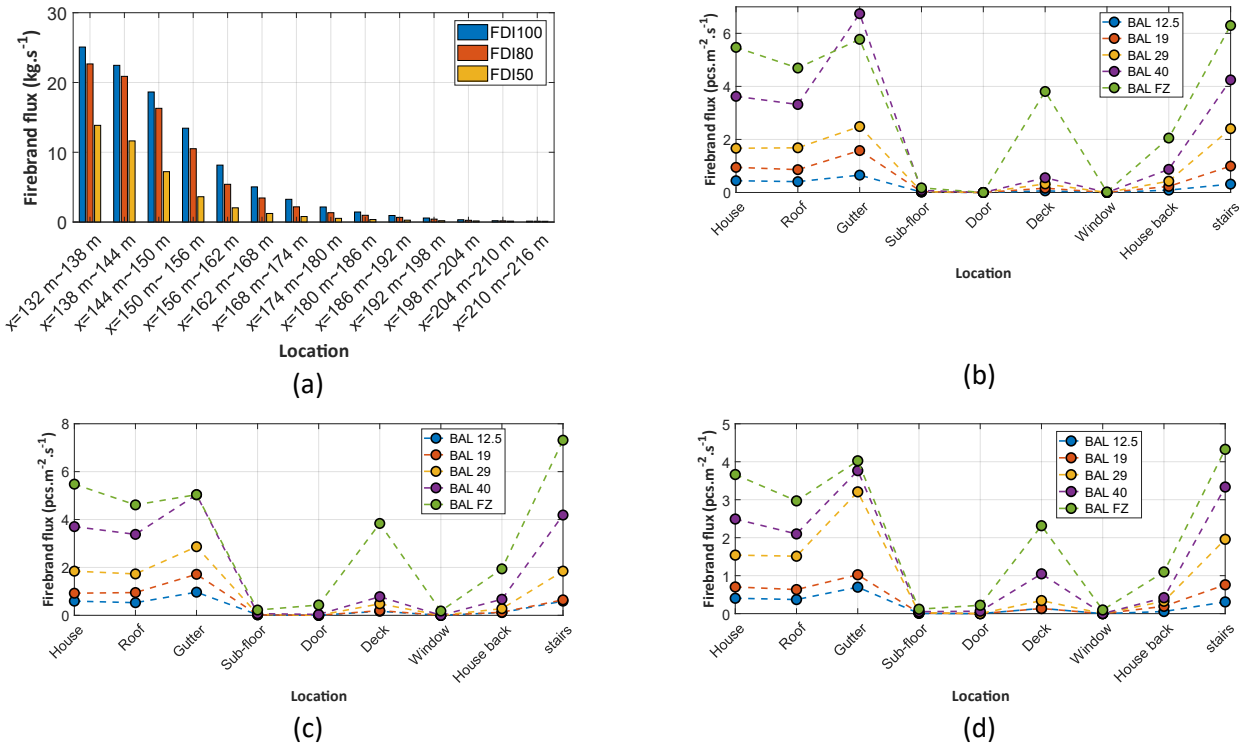

Fig. 2 (a) Firebrand mass distribution in the downwind direction. Firebrand flux on strategic locations of the house (a) FFDI 100, (b) FFDI 80, and (c) FFDI 50.

Fig. 2 (b), (c) and (d) present the firebrand flux on the strategic locations of the house for BALs and FFDIs of 100, 80, and 50. The gutters, roof, deck and stairs are the most vulnerable locations while the sub-floor, window and the back of the house show relatively lower firebrand flux. In other words, the places that are close to fire flame and exposed to wind flow have received more firebrands compared to the places that are not. The firebrand flux decreases with the FFDI at every location. This behaviour is similar for BALs except between BAL FZ and BAL 40 in FFDI 100. The reason for this behaviour could be contacting the fire flame with the house in BAL FZ of FFDI 100, which creates a complex nature for firebrand attack compared to the other occasions.

The correlations between firebrand flux and the radiative heat flux are shown in Fig. 3 for the FFDIs. There is a logarithmic relationship between these two parameters with an agreement of $R^2 > 0.96$. When the house locates away from the fireline, the firebrand flux and the radiative heat flux values are decreasing and converge for FFDIs showing a lower risk to the house. The correlations are useful to find the firebrand and radiative heat flux on the house which is going to construct at a known distance to a forest.

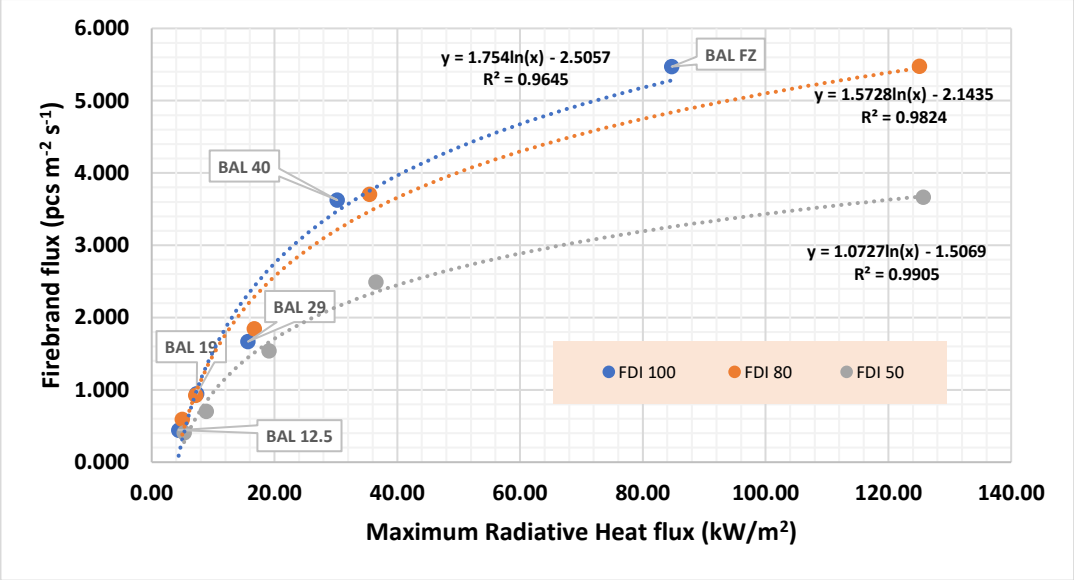

Fig. 3 Firebrand flux against the radiative heat flux on the house for FFDI 100, 80, and 50.

Conclusion

A series of physics-based simulations are conducted to quantify the firebrand and radiative heat flux on a structure in a Eucalyptus dominant WUI. The firebrand generation rates are calculated according to the FFDI, accounting for the effects of fuel species, wind speed, and FMC. The firebrand and heat flux on a modelled house are quantified and found a logarithmic correlation between them. Having such quantification of firebrand attack correlated to the current radiation heat flux of BAL is important to implement the existing AS3959 building standard to improve the construction requirements of buildings in bushfire-prone areas in Australia.

References

1. Manzello, S.L.; Cleary, T.G.; Shields, J.R.; Maranghides, A.; Mell, W.; Yang, J.C. Experimental investigation of firebrands: generation and ignition of fuel beds. *Fire Safety Journal* **2008**, *43*, 226-233.
2. Maranghides, A.; Mell, W. A case study of a community affected by the Witch and Guejito wildland fires. *Fire technology* **2011**, *47*, 379-420.
3. Leonard, J.; Blanchi, R.; Bowditch, P. Bushfire impact from a house's perspective. In Proceedings of the Earth Wind and Fire–Bushfire 2004 Conference, Adelaide, 2004.
4. Intini, P.; Ronchi, E.; Gwynne, S.; Benichou, N. Guidance on design and construction of the built environment against wildland-urban interface fire hazard: a review. *Fire technology* **2020**, *56*, 1853-1883.
5. Government, A. *FireSmart Guide book for community protection, A Guidebook for Wildland/Urban interface communities*; Alberta Government: 2013.
6. Cohen, J.D. Preventing disaster: home ignitability in the wildland-urban interface. *Journal of Forestry* **2000**, *98*, 15-21.
7. Government, N.Z. *Fire and Emergency New Zealand Act 2017*; 2017.
8. Bovio, G.; Camia, A.; MarzanoR, P.D. Prevenzione antincendi boschivi in zona di interfaccia urbano foresta. *Universitadi Torino–Regione Piemonte* **2001**.
9. Francaise, R. Code forestier. **2017**.

10. Weir, I. AS 3959: 2018: Construction of buildings in bushfire-prone areas: Standards Australia. **2018**.
11. McGrattan, K.; Hostikka, S.; McDermott, R.; Floyd, J.; Weinschenk, C.; Overholt, K.J.N.s.p. Fire dynamics simulator technical reference guide volume 1: mathematical model. **2013**, *1018*, 175.
12. Jarrin, N.; Benhamadouche, S.; Laurence, D.; Prosser, R. A synthetic-eddy-method for generating inflow conditions for large-eddy simulations. *International Journal of Heat Fluid Flow* **2006**, *27*, 585-593.
13. Wickramasinghe, A.; Khan, N.; Moinuddin, K. Determining firebrand generation rate using physics-based modelling from experimental studies through inverse analysis. *Fire* **2022**, *5*, 6.
14. Noble, I.; Gill, A.; Bary, G. McArthur's fire-danger meters expressed as equations. *Australian Journal of Ecology* **1980**, *5*, 201-203.
15. Wadhwani, R. Physics-based simulation of short-range spotting in wildfires. Victoria University, 2019.
16. Moinuddin, K.; Sutherland, D.J.M.; Simulation, C.i. Modelling of tree fires and fires transitioning from the forest floor to the canopy with a physics-based model. **2020**, *175*, 81-95.
17. Hudson, T.R.; Bray, R.B.; Blunck, D.L.; Page, W.; Butler, B. Effects of fuel morphology on ember generation characteristics at the tree scale. *International Journal of Wildland Fire* **2020**, *29*, 1042-1051.
18. Bahrani, B. Characterization of Firebrands Generated from Selected Vegetative Fuels in Wildland Fires. The University of North Carolina at Charlotte, 2020.
19. Home, Y. Australia's Guide to Environmentally Sustainable Homes. Available online: https://www.yourhome.gov.au/house-designs (accessed on 14th May).